

1 Inferring the effective start dates of non-pharmaceutical
2 interventions during COVID-19 outbreaks

3 Ilia Kohanovski¹, Uri Obolski^{2,3}, and Yoav Ram^{1,a}

4 ¹School of Computer Science, Interdisciplinary Center Herzliya, Herzliya 4610101, Israel

5 ²School of Public Health, Tel Aviv University, Tel Aviv 6997801, Israel

6 ³Porter School of the Environment and Earth Sciences, Tel Aviv University, Tel Aviv 6997801, Israel

7 ^aCorresponding author: yoav@yoavram.com

8 May 24, 2020

9 **Abstract**

10 During February and March 2020, several countries implemented non-pharmaceutical inter-
11 ventions, such as school closures and lockdowns, with variable schedules to control the COVID-19
12 pandemic caused by the SARS-CoV-2 virus. Overall, these interventions seem to have success-
13 fully reduced the spread of the pandemic. We hypothesise that the official and effective start date
14 of such interventions can significantly differ, for example due to slow adoption by the population,
15 or due to unpreparedness of the authorities and the public. We fit an SEIR model to case data
16 from 12 countries to infer the effective start dates of interventions and contrast them with the
17 official dates. We find both late and early effects of interventions. For example, Italy implemented
18 a nationwide lockdown on Mar 11, but we infer the effective date on Mar 16 (± 0.47 days 95% CI).
19 In contrast, Spain announced a lockdown on Mar 14, but we infer an effective start date on Mar 8
20 or 9 (± 1.08 days 95% CI). We discuss potential causes and consequences of our results.

21 Introduction

22 The COVID-19 pandemic has resulted in implementation of extreme non-pharmaceutical interventions
23 (NPIs) in many affected countries. These interventions, from social distancing to lockdowns, are
24 applied in a rapid and widespread fashion. NPIs are designed and assessed using epidemiological
25 models, which follow the dynamics of the viral infection to forecast the effect of different mitigation and
26 suppression strategies on the levels of infection, hospitalization, and fatality. These epidemiological
27 models usually assume that the effect of NPIs on disease transmission begins at the officially declared
28 date^{14,9,7}.

29 Adoption of public health recommendations is often critical for effective response to infectious dis-
30 eases, and has been studied in the context of HIV¹³ and vaccination^{4,19}, for example. However,
31 behavioural and social change does not occur immediately, but rather requires time to diffuse in the
32 population through media, social networks, and social interactions. Moreover, compliance to NPIs
33 may differ between different interventions and between people with different backgrounds. For ex-
34 ample, in a survey of 2,108 adults in the UK during Mar 2020, Atchison et al.² found that those
35 over 70 years old were more likely to adopt social distancing than young adults (18-34 years old),
36 and that those with lower income were less likely to be able to work from home and to self-isolate.
37 Similarly, compliance to NPIs may be impacted by personal experiences. Smith et al.¹⁶ have surveyed
38 6,149 UK adults in late April and found that people who believe they have already had COVID-19
39 are more likely to think they are immune, and less likely to comply with social distancing measures.
40 Compliance may also depend on risk perception as perceived by the the number of domestic cases or
41 even by reported cases in other regions and countries. Interestingly, the perceived risk of COVID-19
42 infection has likely caused a reduction in the number of influenza-like illness cases in the US starting
43 from mid-February²⁰.

44 Here, we hypothesize that there is a significant difference between the official start of NPIs and their
45 adoption by the public and therefore their effect on transmission dynamics. We use a *Susceptible-*
46 *Exposed-Infected-Recovered* (SEIR) epidemiological model and *Markov Chain Monte Carlo* (MCMC)
47 parameter estimation framework to infer the effective start date of NPIs from publicly available
48 COVID-19 case data in several geographical regions. We compare these estimates to the official dates,
49 and find that they include both late and early effects of NPIs on COVID-19 transmission dynamics.
50 We conclude by demonstrating how differences between the official and effective start of NPIs can
51 confuse assessments of the effectiveness of the NPIs in a simple epidemic control framework.

52 Models and Methods

53 **Data.** We use daily confirmed case data $\mathbf{X} = (X_1, \dots, X_T)$ from 12 regions. These incidence data
54 summarise the number of individuals X_t tested positive for SARS-CoV-2 RNA (using RT-qPCR) at
55 each day t . Data for Wuhan, China retrieved from Pei and Shaman¹⁵, data for 11 European countries
56 retrieved from Flaxman et al.⁷. Regions in which there were multiple sequences of days with zero
57 confirmed cases (e.g. France), we cropped the data to begin with the last sequence so that our analysis
58 focuses on the first sustained outbreak rather than isolated imported cases. For dates of official NPI
59 dates see Table 1.

60 **SEIR model.** We model SARS-CoV-2 infection dynamics by following the number of susceptible
61 S , exposed E , reported infected I_r , and unreported infected I_u individuals in a population of size N .
62 This model distinguishes between reported and unreported infected individuals: the reported infected
63 are those that have enough symptoms to eventually be tested and thus appear in daily case reports, to
64 which we fit the model.

Country	First	Last
Austria	Mar 10 2020	Mar 16 2020
Belgium	Mar 12 2020	Mar 18 2020
Denmark	Mar 12 2020	Mar 18 2020
France	Mar 13 2020	Mar 17 2020
Germany	Mar 12 2020	Mar 22 2020
Italy	Mar 5 2020	Mar 11 2020
Norway	Mar 12 2020	Mar 24 2020
Spain	Mar 9 2020	Mar 14 2020
Sweden	Mar 12 2020	Mar 18 2020
Switzerland	Mar 13 2020	Mar 20 2020
United Kingdom	Mar 16 2020	Mar 24 2020
Wuhan	Jan 23 2020	Jan 23 2020

Table 1: Official start of non-pharmaceutical interventions. The date of the first intervention is for a ban of public events, or encouragement of social distancing, or for school closures. In all countries except Sweden, the date of the last intervention is for a lockdown. In Sweden, where a lockdown was not ordered during the studied dates, the last date is for school closures. Dates for European countries from Flaxman et al.⁷, date for Wuhan, China from Pei and Shaman¹⁵. See Figure 1 for a visual presentation.

65 Susceptible (S) individuals become exposed due to contact with reported or unreported infected
 66 individuals (I_r or I_u) at a rate β_t or $\mu\beta_t$. The parameter $0 < \mu < 1$ represents the decreased transmission
 67 rate from unreported infected individuals, who are often subclinical or even asymptomatic^{17,6}. The
 68 transmission rate $\beta_t \geq 0$ may change over time t due to behavioural changes of both susceptible
 69 and infected individuals. Exposed individuals, after an average incubation period of Z days, become
 70 reported infected with probability α_t or unreported infected with probability $(1 - \alpha_t)$. The reporting
 71 rate $0 < \alpha_t < 1$ may also change over time due to changes in human behavior. Infected individuals
 72 remain infectious for an average period of D days, after which they either recover, or becomes ill
 73 enough to be quarantined. They therefore no longer infect other individuals, and the model does not
 74 track their frequency. The model is described by the following equations:

$$\begin{aligned}
 \frac{dS}{dt} &= -\beta_t S \frac{I_r}{N} - \mu\beta_t S \frac{I_u}{N} \\
 \frac{dE}{dt} &= \beta_t S \frac{I_r}{N} + \mu\beta_t S \frac{I_u}{N} - \frac{E}{Z} \\
 \frac{dI_r}{dt} &= \alpha_t \frac{E}{Z} - \frac{I_r}{D} \\
 \frac{dI_u}{dt} &= (1 - \alpha_t) \frac{E}{Z} - \frac{I_r}{D} \\
 \frac{dR}{dt} &= \frac{I_r}{D} + \frac{I_r}{D}.
 \end{aligned} \tag{1}$$

75

76 The initial numbers of exposed $E(0)$ and unreported infected $I_u(0)$ are free model parameters (i.e.
 77 estimated during model fitting), whereas the initial number of reported infected is assumed to be
 78 zero $I_r(0) = 0$, and the number of susceptible is $S(0) = N - E(0) - I_u(0)$. This model is inspired
 79 by Li et al.¹⁴ and Pei and Shaman¹⁵, who used a similar model with multiple regions and constant
 80 transmission β and reporting rate α to infer COVID-19 dynamics in China and the continental US,
 81 respectively.

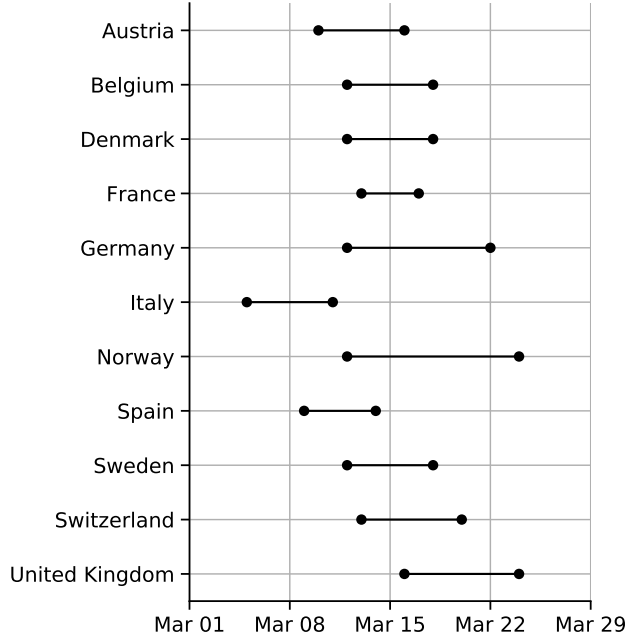


Figure 1: Official start of non-pharmaceutical interventions. See Table 1 for more details. Wuhan, China is not shown.

82 **Likelihood function.** For a given vector θ of model parameters the *expected* cumulative number of
83 reported infected individuals (I_r) until day t is, following Eq. (1),

$$84 \quad Y_t(\theta) = \int_0^t \alpha_s \frac{E(s)}{Z} ds, \quad Y_0 = 0. \quad (2)$$

85 We assume that reported infected individuals are confirmed and therefore observed in the daily case
86 report of day t with probability p_t (note that an individual can only be observed once, and that p_t may
87 change over time, but t is a specific date rather than the time elapsed since the individual was infected).
88 We denote by X_t the *observed* number of confirmed cases in day t , and by \tilde{X}_t the cumulative number
89 of confirmed cases until end of day t ,

$$90 \quad \tilde{X}_t = \sum_{i=1}^t X_i. \quad (3)$$

91 Therefore, at day t the number of reported infected yet-to-be confirmed individuals is $(Y_t(\theta) - \tilde{X}_{t-1})$.
92 We therefore assume that X_t conditioned on \tilde{X}_{t-1} is Poisson distributed,

$$93 \quad \begin{aligned} (X_1 \mid \theta) &\sim Poi(Y_1(\theta) \cdot p_1), \\ (X_t \mid \tilde{X}_{t-1}, \theta) &\sim Poi((Y_t(\theta) - \tilde{X}_{t-1}) \cdot p_t), \quad t > 1. \end{aligned} \quad (4)$$

94 Hence, the *likelihood function* $\mathbb{L}(\theta \mid \mathbf{X})$ for the parameter vector θ given the confirmed case data
95 $\mathbf{X} = (X_1, \dots, X_T)$ is defined by the probability to observe \mathbf{X} given θ ,

$$96 \quad \mathbb{L}(\theta \mid \mathbf{X}) = P(\mathbf{X} \mid \theta) = P(X_1 \mid \theta) \cdot P(X_2 \mid \tilde{X}_1, \theta) \cdots P(X_T \mid \tilde{X}_{T-1}, \theta). \quad (5)$$

97 **NPI model.** To model non-pharmaceutical interventions (NPIs), we set the beginning of the NPIs
98 to day τ and define

$$99 \quad \beta_t = \begin{cases} \beta, & t < \tau \\ \beta\lambda, & t \geq \tau \end{cases}, \quad \alpha_t = \begin{cases} \alpha_1, & t < \tau \\ \alpha_2, & t \geq \tau \end{cases}, \quad p_t = \begin{cases} 1/9, & t < \tau \\ 1/6, & t \geq \tau \end{cases}, \quad (6)$$

100 where $0 < \lambda < 1$. The values for p_t follow Li et al.¹⁴, who estimated the average time between
 101 infection and reporting in Wuhan, China, at 9 days before the start of NPIs and 6 days after start of
 102 NPIs.

103 **Parameter estimation.** To estimate the model parameters from the daily case data \mathbf{X} , we apply a
 104 Bayesian inference approach. We start our model Δt days⁹ before the outbreak (defined as consecutive
 105 days with increasing confirmed cases) in each country. The model in Eq. (1) is parameterized by the
 106 vector θ , where

107
$$\theta = (Z, D, \mu, \{\beta_t\}, \{\alpha_t\}, \{p_t\}, E(0), I_u(0), \tau, \Delta t). \quad (7)$$

108 The likelihood function is defined in Eq. (5). The posterior distribution of the model parameters
 109 $P(\theta | \mathbf{X})$ is estimated using an *affine-invariant ensemble sampler for Markov chain Monte Carlo*
 110 (MCMC)¹¹ implemented in the emcee Python package⁸.

111 We defined the following prior distributions on the model parameters $P(\theta)$:

$$\begin{aligned} Z &\sim \text{Uniform}(2, 5) \\ D &\sim \text{Uniform}(2, 5) \\ \mu &\sim \text{Uniform}(0.2, 1) \\ \beta &\sim \text{Uniform}(0.8, 1.5) \\ \lambda &\sim \text{Uniform}(0, 1) \\ \alpha_1, \alpha_2 &\sim \text{Uniform}(0.02, 1) \\ E(0) &\sim \text{Uniform}(0, 3000) \\ I_u(0) &\sim \text{Uniform}(0, 3000) \\ \Delta t &\sim \text{Uniform}(1, 5) \\ \tau &\sim \text{TruncatedNormal}\left(\frac{\tau^* + \tau^0}{2}, \frac{\tau^* - \tau^0}{2}, 1, T - 2\right), \end{aligned} \quad (8)$$

112 where the prior for τ is a truncated normal distribution shaped so that the date of the first and last NPI,
 113 τ^0 and τ^* (Table 1), are at minus and plus one standard deviation, and taking values only between
 114 1 and $T - 2$, where T is the number of days in the data \mathbf{X} . We have also tested an uninformative
 115 uniform prior $U(1, T - 2)$. The uninformative prior could result in non-negligible posterior probability
 116 for unreasonable τ values, such as Mar 1 in the United Kingdom. This was probably due to MCMC
 117 chains being stuck in low posterior regions of the parameter space. We therefore decided to use the
 118 more informative truncated normal prior. Other priors follow Li et al.¹⁴, with the following exceptions.
 119 λ is used to ensure transmission rates are lower after the start of the NPIs ($\lambda < 1$). We checked values
 120 of Δt larger than five days and found they generally produce lower likelihood, higher DIC (see below),
 121 and unreasonable parameter estimates, and therefore chose $U(1, 5)$ as the prior.

123 **Model comparison.** We perform model selection using two methods. First, we compute WAIC
 124 (widely applicable information criterion)¹⁰,

125
$$WAIC(\theta, \mathbf{X}) = -2 \log \mathbb{E}[\mathcal{L}(\theta | \mathbf{X})] + 2\mathbb{V}[\log \mathcal{L}(\theta | \mathbf{X})] \quad (9)$$

126 where $\mathbb{E}[\cdot]$ and $\mathbb{V}[\cdot]$ are the expectation and variance operators taken over the posterior distribution
 127 $P(\theta | \mathbf{X})$. We compare models by reporting their relative WAIC; lower is better (Table S1). A
 128 minority (<5%) of MCMC chains that fail to fully converge can lead to overestimation of the variance
 129 (the second term in Eq. (9)). Therefore, we exclude from the WAIC computation chains with mean
 130 log-likelihood that is three standard deviations or more from the overall mean.

131 We also plot posterior predictions: we sample 1,000 parameter vectors from the posterior distribution
 132 $P(\theta | \mathbf{X})$, use these parameter vectors to simulate the SEIR model (Eq. (1)), and plot the simulated
 133 dynamics (Figure S3a). Both the accuracy (i.e. overlap of data and prediction) and the precision (i.e.
 134 the compactness of the predictions) are good ways to visually compare models.

135 **Source code.** We use Python 3 with the NumPy, Matplotlib, SciPy, Pandas, Seaborn, and emcee
 136 packages. All source code will be publicly available under a permissive open-source license at
 137 github.com/yoavram-lab/EffectiveNPI. Samples from the posterior distributions will be deposited on
 138 FigShare.

139 Results

140 Several studies have described the effects of non-pharmaceutical interventions in different geographical
 141 regions^{7,9,14}. These studies have assumed that the parameters of the epidemiological model change
 142 at a specific date, as in Eq. (6), and set the change date τ to the official NPI date τ^* (Table 1). They
 143 then fit the model once for time $t < \tau^*$ and once for time $t \geq \tau^*$. For example, Li et al.¹⁴ estimate
 144 the dynamics in China before and after τ^* at Jan 23. Thereby, they effectively estimate (β, α_1) and
 145 (λ, α_2) separately. Here we estimate the posterior distribution $P(\tau | \mathbf{X})$ of the *effective* start date of the
 146 NPIs by jointly estimating $\tau, \beta, \lambda, \alpha_1, \alpha_2$ on the entire data per region (e.g. Italy, Austria), rather than
 147 splitting the data at τ^* . We then estimate the posterior probability $P(\tau | \mathbf{X})$ by marginalizing the joint
 148 posterior, and estimate $\hat{\tau}$ as the posterior median.

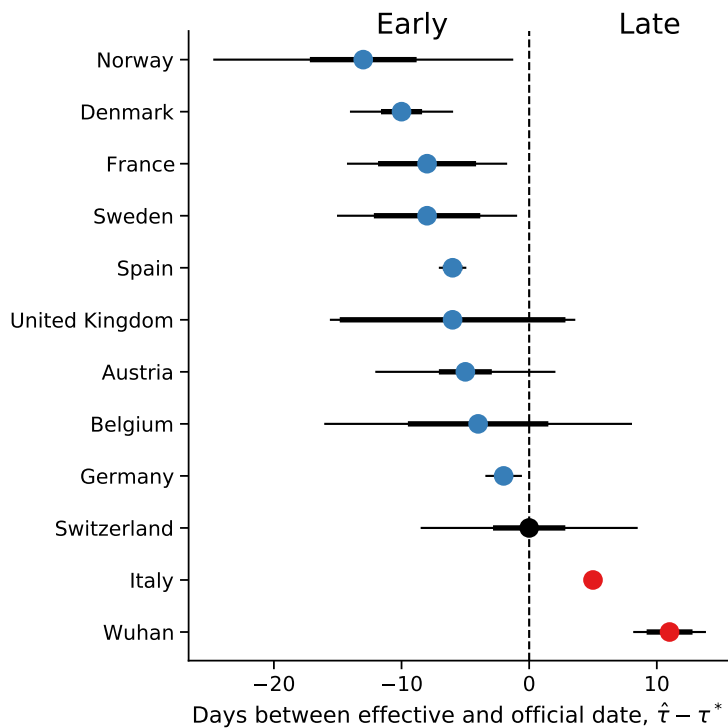


Figure 2: Official vs. effective start of non-pharmaceutical interventions. The difference between $\hat{\tau}$ the
 effective and τ^* the official start of NPI is shown for different regions. The effective NPI dates in Italy and Wuhan
 are significantly delayed compared to the official dates, whereas in Denmark, France, Spain, and Germany, the
 effective date is earlier than the official date. $\hat{\tau}$ is the posterior median, see Table 2. τ^* is the last NPI date,
 see Table 1. Thin and bold lines show 95% and 75% credible intervals, respectively (i.e. area in which
 $P(|\tau - \hat{\tau}| | \mathbf{X}) = 0.95$ and 0.75 .)

149 We compared the posterior predictive plots of a model with a free τ with those of a model with τ fixed
 150 at τ^* and without τ . The model with free τ clearly produces better and less variable predictions (Figure
 151 S3a). When we compared the models using WAIC (Table S1), the model with a free parameter for
 152 the start of the NPI was preferred over the other models in 8 out of 12 of the regions (although only
 153 narrowly for 5 of the 8); the exceptions are Austria, Belgium, Norway, and United Kingdom.

154 We compare the official τ^* and effective $\hat{\tau}$ start of NPIs and find that in most regions the effective start
 155 of NPI significantly differs from the official date (Figure 2), that is, the credible interval on $\hat{\tau}$ does
 156 not include τ^* (Figure 2). The exceptions are, as with the comparison to the simpler models, Austria,
 157 Belgium, and United Kingdom, as well another country (see below). Norway also has a relatively
 158 wide credible interval, which could be expected as it has the longest duration between the first and last
 159 NPIs (Table 1). In the following, we describe our findings on late and early effective start of NPI in
 160 detail.

161 **Late effective start of NPIs.** In both Wuhan, China, and in Italy we find that our estimated effective
 162 start of NPI $\hat{\tau}$ is significantly later than the official date τ^* (Figure 2).

163 In Italy, the first case was officially confirmed on Feb 21. School closures were implemented on
 164 Mar 5⁷, a lockdown was declared in Northern Italy on Mar 8, with social distancing implemented in
 165 the rest of the country, and the lockdown was extended to the entire nation on Mar 11⁹. That is, the
 166 first and last official dates are Mar 8 and Mar 11. However, we estimate the effective date $\hat{\tau}$ at Mar 16
 167 (± 0.47 days 95% CI ; Figure 3).

168 Similarly, in Wuhan, China, a lockdown was ordered on Jan 23¹⁴, but we estimate the effective start
 169 of NPIs to be more than a week later at Feb 2 (± 2.85 days 95% CI Figure 3).

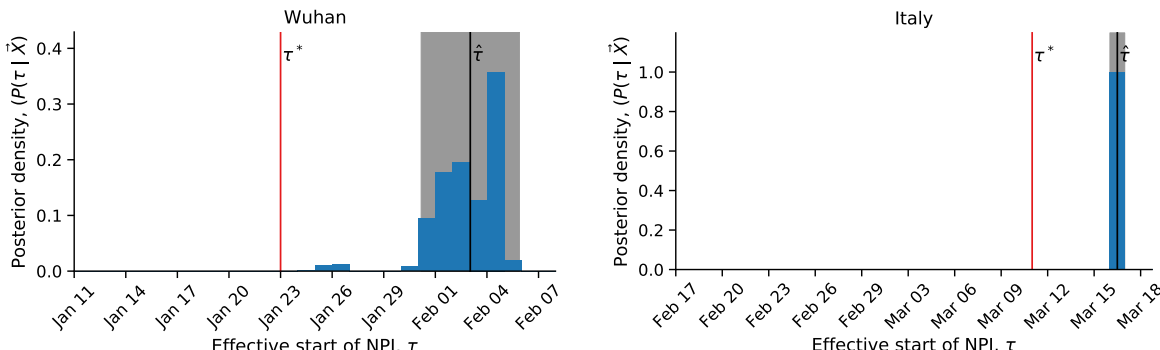


Figure 3: Late effect of non-pharmaceutical interventions in Italy and Wuhan, China. Posterior distribution of τ , the effective start date of NPI, is shown as a histogram of MCMC samples. Red line shows the official last NPI date τ^* . Black line shows the estimated $\hat{\tau}$. Shaded area shows a 95% credible interval (area in which $P(|\tau - \hat{\tau}| | \mathbf{X}) = 0.95$).

170 **Early effective start of NPIs.** In contrast, in some regions we estimate an effective start of NPIs $\hat{\tau}$
 171 that is *earlier* than the official date τ^* (Figure 2). In Spain, social distancing was encouraged starting
 172 on Mar 8⁷, but mass gatherings still occurred on Mar 8, including a march of 120,000 people for the
 173 International Women's Day, and a football match between Real Betis and Real Madrid (2:1) with a
 174 crowd of 50,965 in Seville. A national lockdown was only announced on Mar 14⁷. Nevertheless,
 175 we estimate the effective start of NPI $\hat{\tau}$ on Mar 8 or 9 (± 1.08 days 95%CI), rather than Mar 14
 176 (Figure 4).

177 Similarly, in France we estimate the effective start of NPIs $\hat{\tau}$ on Mar 8 or Mar 9 (± 6.27 days 95% CI,
 178 Figure 4). Although the credible interval is wider compared to Spain, spanning from Mar 2 to Mar 15,

179 the official lockdown start at Mar 17 is later still, and even the earliest NPI, banning of public events,
180 only started on Mar 13⁷.

181 Interestingly, the effective start of NPIs $\hat{\tau}$ in both France and Spain is estimated at Mar 8, although
182 the official NPI dates differ significantly: the first NPI in France is only one day before the last NPI in
183 Spain. The number of daily cases was similar in both countries until Mar 8, but diverged by Mar 13,
184 reaching significantly higher numbers in Spain (Figure S1). This may suggest that correlation exist
185 between effective start of NPIs due to global or international events.

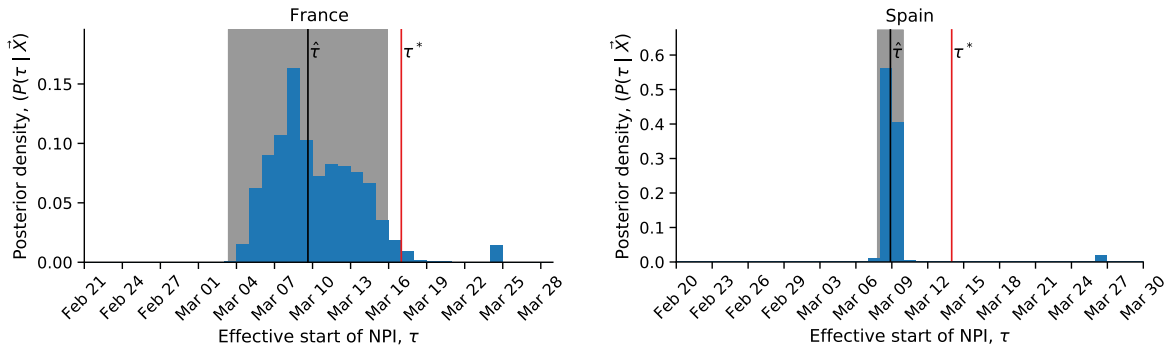


Figure 4: Early effect of non-pharmaceutical interventions in France and Spain. Posterior distribution of τ , the effective start date of NPI, is shown as a histogram of MCMC samples. Red line shows the official last NPI date τ^* . Black line shows the estimated $\hat{\tau}$. Shaded area shows a 95% credible interval (area in which $P(|\tau - \hat{\tau}| \mid \mathbf{X}) = 0.95$).

186 **Like a Swiss watch.** We find one case in which the official and effective dates match: Switzerland
187 ordered a national lockdown on Mar 20, after banning public events and closing schools on Mar 13
188 and 14⁷. Indeed, the posterior median $\hat{\tau}$ is Mar 20 (± 8.46 days 95% CI), and the posterior distribution
189 shows two density peaks: a smaller one between Mar 10 and Mar 14, and a bigger one between Mar 17
190 and Mar 22 (Figure S2). It's also worth mentioning that Switzerland was the first to mandate self
191 isolation of confirmed cases⁷.

Country	τ^*	τ	$CI_{75\%}$	$CI_{95\%}$	Z	D	μ	β	α_1	λ	α_2	$E(0)$	$I_u(0)$	Δt
Austria	Mar 16	Mar 11	2.0738	7.0564	3.9173	3.5938	0.4306	1.0991	0.0568	0.7332	0.4525	464.2434	555.9752	2.4968
Belgium	Mar 18	Mar 14	5.5022	12.0557	3.9515	3.5630	0.4287	1.0943	0.2191	0.8420	0.4308	364.7264	464.5402	2.3387
Denmark	Mar 18	Mar 08	1.6102	4.0409	3.9635	3.4684	0.3749	1.0569	0.0430	0.3163	0.5272	501.8609	638.7421	2.4313
France	Mar 17	Mar 09	3.8404	6.2746	4.0014	3.7026	0.5588	1.1352	0.1972	0.6571	0.4537	530.9004	607.6622	1.9903
Germany	Mar 22	Mar 20	0.4000	1.4323	3.7674	4.0531	0.7504	1.2148	0.3014	0.8036	0.1173	178.6430	112.0369	2.4395
Italy	Mar 11	Mar 16	0.3741	0.4757	4.1638	2.7860	0.5034	0.9971	0.5262	0.4595	0.5347	935.3436	1928.8841	1.6988
Norway	Mar 24	Mar 11	4.1819	11.7512	4.0416	3.4597	0.4132	1.0690	0.1278	0.6774	0.2723	353.4045	486.7205	2.3390
Spain	Mar 14	Mar 08	0.7610	1.0772	3.9399	3.6171	0.6061	1.1102	0.0688	0.7278	0.5331	898.0345	897.6081	2.3740
Sweden	Mar 18	Mar 10	4.1678	7.0558	4.0215	3.4969	0.4176	1.0593	0.1126	0.6376	0.2501	386.2140	494.3708	2.2410
Switzerland	Mar 20	Mar 20	2.8318	8.5025	3.9463	3.7430	0.6164	1.1103	0.1777	0.4682	0.2108	203.2171	230.4321	2.0427
United Kingdom	Mar 24	Mar 18	8.8413	9.6141	3.9799	3.8158	0.5355	1.1464	0.2102	0.8349	0.3894	268.7645	260.6807	2.0749
Wuhan, China	Jan 23	Feb 03	1.7984	2.8493	3.7326	3.6320	0.6057	1.1453	0.2754	0.1784	0.3511	597.8676	561.1586	2.4248

Table 2: Parameter estimates for different regions. See Eq. (1) for model parameters. All estimates are posterior medians. 75% and 95% credible intervals given for τ , in days. τ^* is the official last NPI date, see Table 1.

192 **Consequences of late and early effect of NPIs on real-time assessment.** The success of non-
 193 pharmaceutical interventions is assessed by health officials using various metrics, such as the decline
 194 in the growth rate of daily cases. These assessments are made a specific number of days after the
 195 intervention began, to accommodate for the expected serial interval³ (i.e. time between successive
 196 cases in a chain of transmission), which is estimated at about 4-7 days⁹.

197 However, a significant difference between the beginning of the intervention and the effective change in
 198 transmission rates can invalidate assessments that assume a serial interval of 4-7 days and neglect the
 199 late or early population response to the NPI. This is illustrated in Figure 5 using data and parameters
 200 from Italy. Here, a lockdown is officially ordered on Mar 10 (τ^*), but its late effect on the transmission
 201 dynamics starts on Mar 16 ($\hat{\tau}$). If health officials assume the dynamics to immediately change at τ^* ,
 202 they will expect the number of cases be within the red lines (posterior predictions assuming $\tau = \tau^*$).
 203 This leads to a significant underestimation, which might be interpreted by officials as ineffectiveness
 204 of NPIs, leading to further escalations. However, the number of cases will actually follow the blue
 205 lines (posterior predictions using $\tau = \hat{\tau}$), which corresponds well to the real data.

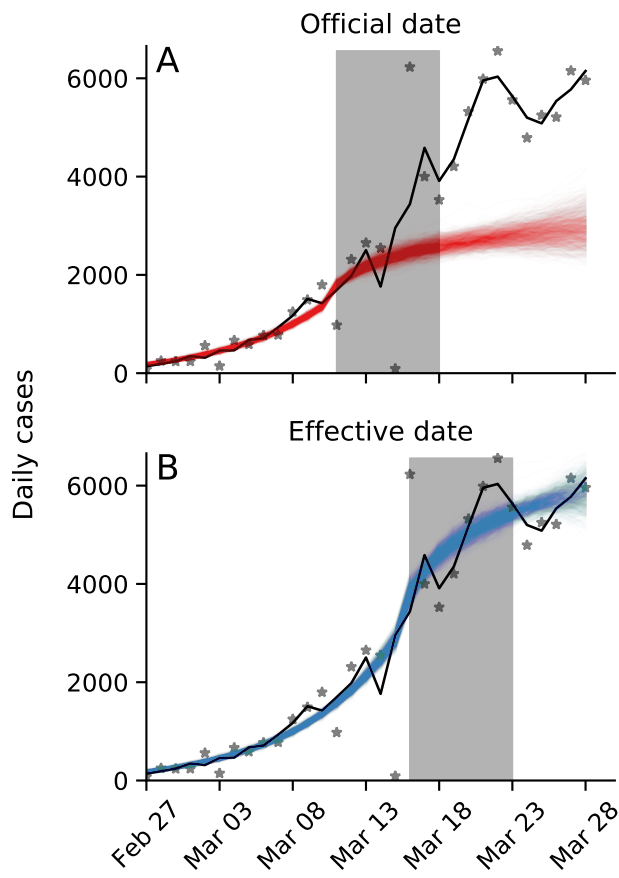


Figure 5: Late effective start of NPIs leads to under-estimation of daily confirmed cases. Real number of daily cases in Italy in black (markers: data, line: time moving average). Model posterior predictions are shown as coloured lines (1,000 draws from the posterior distribution). Shaded box illustrates a serial interval of seven days. **(A)** Using the official date τ^* for the start of the NPI, the model under-estimates the number of cases seven days after the start of the NPI. **(B)** Using the effective date $\hat{\tau}$ for the start of the NPI, the model correctly estimates the number of cases seven days after the start of the NPI. Here, model parameters are estimates for Italy (Table 2).

206 **Discussion**

207 We have estimated the effective start date of NPIs in several geographical regions using an SEIR
208 epidemiological model and an MCMC parameter estimation framework. We find examples of both
209 late and early effect of NPIs (Figure 2).

210 For example, in Italy and Wuhan, China, the effective start of the lockdowns seems to have occurred
211 more than five days after the official date (Figure 3). This difference might be explained by low
212 compliance: In Italy, for example, the government intention to lockdown Northern provinces leaked
213 to the public, resulting in people leaving those provinces⁹. Late effect of NPIs might also be due to
214 the time required by both the government and the citizens to organise for a lockdown, and for the new
215 guidelines to diffuse in the population.

216 In contrast, in most investigated countries (e.g., Spain and France), we infer reduced transmission rates
217 even before official lockdowns were implemented (Figure 4). An early effective date might be due
218 to early adoption of social distancing and similar behavioural adaptations in parts of the population.
219 These behavioural adaptations may have a stronger influence than previously thought. In addition,
220 diffusion of these behaviours may occur via media and social networks, rather than official government
221 recommendations and instructions, and may have been influenced by increased risk perception due
222 to domestic or international COVID-19-related reports. Indeed, the evidence supports a change in
223 transmission dynamics (i.e. a model with free τ) even for Sweden (Figure S3a), in which a lockdown
224 was not implemented*.

225 Attempts to asses the effect of NPIs^{7,3} generally assume a seven-day delay between the implementation
226 of the intervention and the observable change in dynamics, due to the characteristic serial interval of
227 COVID-19⁹. However, the late and early effects we have estimated may bias these assessments and
228 lead to wrong conclusions about the effects of NPIs (Figure 5).

229 We have found that the evidence supports a model in which the parameters change at a specific time
230 point τ over a model without such a change-point in 9 out of 12 regions (Table S1). It could be
231 interesting to check if the evidence favours a model with *two* change-points, rather than one. Two
232 such change-points could reflect escalating NPIs (e.g. school closures followed by lockdowns), or
233 an intervention followed by a relaxation. However, interpretation of such models will be harder, as
234 two change-points can also reflect a mix of NPIs and other events, such as weather, or domestic and
235 international events that affect risk perception.

236 As several countries (e.g. Austria) begin to relieve lockdowns and ease restrictions, we expect similar
237 delays and advances to occur: in some countries people will begin to behave as if restrictions were
238 eased even before the official date, and in some countries people will continue to self-restrict even
239 after restrictions are officially removed.

240 **Conclusions.** We have estimated the effective start date of NPIs and found that they often differ from
241 the official dates. Our results highlight the complex interaction between personal, regional, and global
242 determinants of behavioral response to infectious disease. Therefore, we emphasize the need to further
243 study variability in compliance and behavior over both time and space. This can be accomplished
244 both by surveying differences in compliance within and between populations², and by incorporating
245 specific behavioral models into epidemiological models^{5,18,1}.

*Sweden banned public events on Mar 12, encouraged social distancing on Mar 16, and closed schools on Mar 18⁷.

246 Acknowledgements

247 We thank Lilach Hadany and Oren Kolodny for discussions and comments. This work was supported in part by
248 the Israel Science Foundation 552/19 and 1399/17.

249 References

- [1] Arthur, R. F., Jones, J. H., Bonds, M. H. and Feldman, M. W. 2020, ‘Complex dynamics induced by delayed adaptive behavior during outbreaks’, *bioRxiv* pp. 1–23.
- [2] Atchison, C. J., Bowman, L., Vrinten, C., Redd, R., Pristera, P., Eaton, J. W. and Ward, H. 2020, ‘Perceptions and behavioural responses of the general public during the COVID-19 pandemic: A cross-sectional survey of UK Adults’, *medRxiv* p. 2020.04.01.20050039.
- [3] Banholzer, N., Weenen, E. V., Kratzwald, B. and Seeliger, A. 2020, ‘The estimated impact of non-pharmaceutical interventions on documented cases of COVID-19 : A cross-country analysis’, *medRxiv*.
- [4] Dunn, A. G., Leask, J., Zhou, X., Mandl, K. D. and Coiera, E. 2015, ‘Associations between exposure to and expression of negative opinions about human papillomavirus vaccines on social media: An observational study’, *J. Med. Internet Res.* **17**(6), e144.
- [5] Fenichel, E. P., Castillo-Chavez, C., Ceddia, M. G., Chowell, G., Gonzalez Parrae, P. A., Hickling, G. J., Holloway, G., Horan, R., Morin, B., Perrings, C., Springborn, M., Velazquez, L. and Villalobos, C. 2011, ‘Adaptive human behavior in epidemiological models’, *Proc. Natl. Acad. Sci. U. S. A.* **108**(15), 6306–6311.
- [6] Ferretti, L., Wymant, C., Kendall, M., Zhao, L., Nurtay, A., Abeler-Dörner, L., Parker, M., Bonsall, D. and Fraser, C. 2020, ‘Quantifying SARS-CoV-2 transmission suggests epidemic control with digital contact tracing’, *Science (80-.).* **368**(6491), eabb6936.
- [7] Flaxman, S., Mishra, S., Gandy, A., Unwin, J. T., Coupland, H., Mellan, T. A., Zhu, H., Berah, T., Eaton, J. W., Guzman, P. N. P., Schmit, N., Cilloni, L., Ainslie, K. E. C., Baguelin, M., Blake, I., Boonyasiri, A., Boyd, O., Cattarino, L., Ciavarella, C., Cooper, L., Cucunubá, Z., Cuomo-Dannenburg, G., Dighe, A., Djaafara, B., Dorigatti, I., Van Elsland, S., Fitzjohn, R., Fu, H., Gaythorpe, K., Geidelberg, L., Grassly, N., Green, W., Hallett, T., Hamlet, A., Hinsley, W., Jeffrey, B., Jorgensen, D., Knock, E., Laydon, D., Nedjati-Gilani, G., Nouvellet, P., Parag, K., Siveroni, I., Thompson, H., Verity, R., Volz, E., Gt Walker, P., Walters, C., Wang, H., Wang, Y., Watson, O., Xi, X., Winskill, P., Whittaker, C., Ghani, A., Donnelly, C. A., Riley, S., Okell, L. C., Vollmer, M. A. C., Ferguson, N. M. and Bhatt, S. 2020, ‘Estimating the number of infections and the impact of non-pharmaceutical interventions on COVID-19 in 11 European countries’, *Imp. Coll. London* (March), 1–35.
- [8] Foreman-Mackey, D., Hogg, D. W., Lang, D. and Goodman, J. 2013, ‘emcee : The MCMC Hammer’, *Publ. Astron. Soc. Pacific* **125**(925), 306–312.
- [9] Gatto, M., Bertuzzo, E., Mari, L., Miccoli, S., Carraro, L., Casagrandi, R. and Rinaldo, A. 2020, ‘Spread and dynamics of the COVID-19 epidemic in Italy: Effects of emergency containment measures’, *Proc. Natl. Acad. Sci.* p. 202004978.
- [10] Gelman, A., Carlin, J. B., Stern, H. S., Dunson, D. B., Vehtari, A. and Rubin, D. B. 2013, *Bayesian Data Analysis, Third Edition*, Chapman & Hall/CRC Texts in Statistical Science, Taylor & Francis.

- [11] Goodman, J. and Weare, J. 2010, ‘Ensemble Samplers With Affine Invariance’, *Commun. Appl. Math. Comput. Sci.* **5**(1), 65–80.
- [12] Kass, R. E. and Raftery, A. E. 1995, ‘Bayes Factors’, *J. Am. Stat. Assoc.* **90**(430), 773.
- [13] Kaufman, M. R., Cornish, F., Zimmerman, R. S. and Johnson, B. T. 2014, ‘Health behavior change models for HIV prevention and AIDS care: Practical recommendations for a multi-level approach’, *J. Acquir. Immune Defic. Syndr.* **66**(SUPPL.3), 250–258.
- [14] Li, R., Pei, S., Chen, B., Song, Y., Zhang, T., Yang, W. and Shaman, J. 2020, ‘Substantial undocumented infection facilitates the rapid dissemination of novel coronavirus (SARS-CoV2)’, *Science* (80-.). p. eabb3221.
- [15] Pei, S. and Shaman, J. 2020, ‘Initial Simulation of SARS-CoV2 Spread and Intervention Effects in the Continental US’, *medRxiv* p. 2020.03.21.20040303.
- [16] Smith, L. E., Mottershaw, A. L., Egan, M., Waller, J., Marteau, T. M. and Rubin, G. J. 2020, ‘The impact of believing you have had COVID-19 on behaviour : Cross-sectional survey’, *medRxiv* pp. 1–20.
- [17] Thompson, R. N., Lovell-Read, F. A. and Obolski, U. 2020, ‘Time from Symptom Onset to Hospitalisation of Coronavirus Disease 2019 (COVID-19) Cases: Implications for the Proportion of Transmissions from Infectors with Few Symptoms’, *J. Clin. Med.* **9**(5), 1297.
- [18] Walters, C. E. and Kendal, J. R. 2013, ‘An SIS model for cultural trait transmission with conformity bias’, *Theor. Popul. Biol.* **90**, 56–63.
- [19] Wiyeh, A. B., Cooper, S., Nnaji, C. A. and Wiysonge, C. S. 2018, ‘Vaccine hesitancy ’outbreaks’: using epidemiological modeling of the spread of ideas to understand the effects of vaccine related events on vaccine hesitancy’, *Expert Rev. Vaccines* **17**(12), 1063–1070.
- [20] Zipfel, C. M. and Bansal, S. 2020, ‘Assessing the interactions between COVID-19 and influenza in the United States’, *medRxiv* (February), 1–13.

Supplementary Material

Country	Fixed	Free	No
Austria	26.68	28.40	39.70
Belgium	29.38	30.62	28.80
Denmark	38.56	37.34*	49.63
France	49.90	49.60*	72.17
Germany	214.95	158.90**	310.65
Italy	301.39	233.07**	433.42
Norway	34.04	36.07	37.54
Spain	59.93	59.54*	141.96
Sweden	25.93	25.91*	28.35
Switzerland	74.90	72.97*	99.65
United Kingdom	38.10	37.39	35.77
Wuhan China	94.00	73.75**	107.31

Table S1: WAIC values for the different models. WAIC (widely applicable information criterion)¹⁰ values for models with: no τ at all, *No*; τ fixed at the official last NPI date τ^* , *Fixed*; and free parameter τ , *Free*. WAIC values are scaled as a deviance measure: lower values imply higher predictive accuracy. Bold emphasise cases in which the *Free* model had the lowest WAIC. * and ** mark if the difference was smaller or greater than 2, which is a popular significance level for model comparison¹².

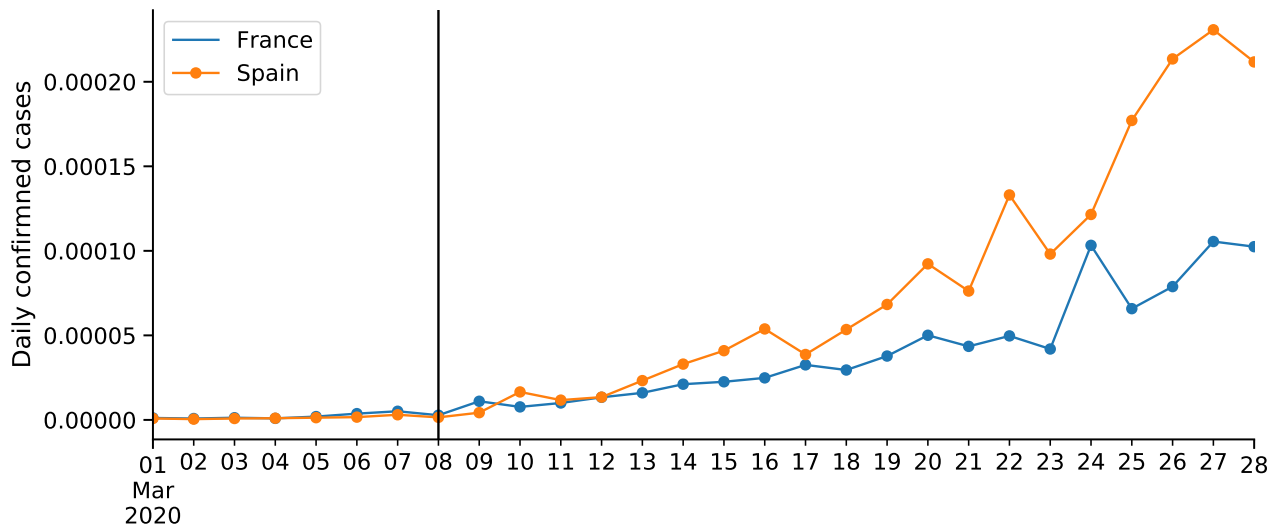


Figure S1: COVID-19 confirmed cases in France and Spain. Number of cases proportional to population size (as of 2018). Vertical line shows Mar 8, the effective start of NPIs $\hat{\tau}$ in both countries.

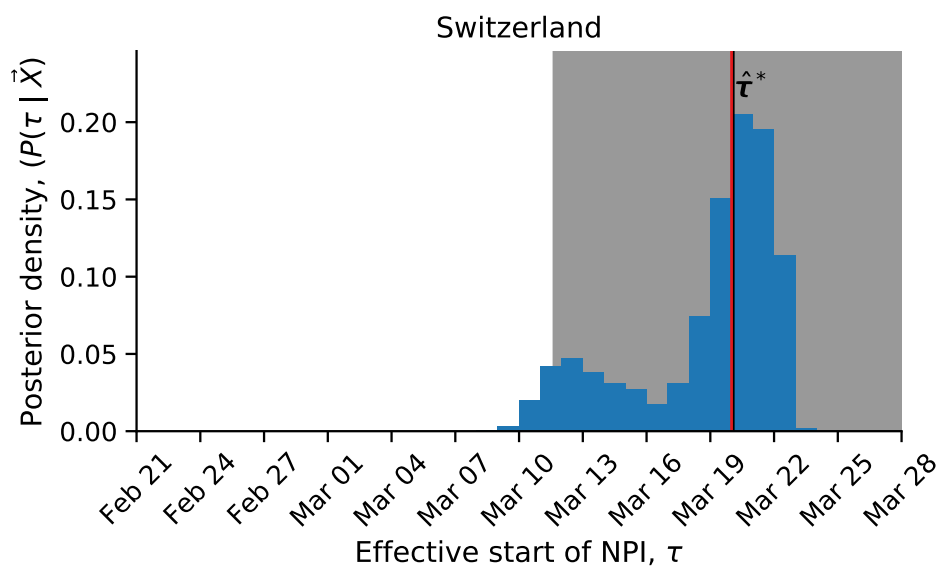
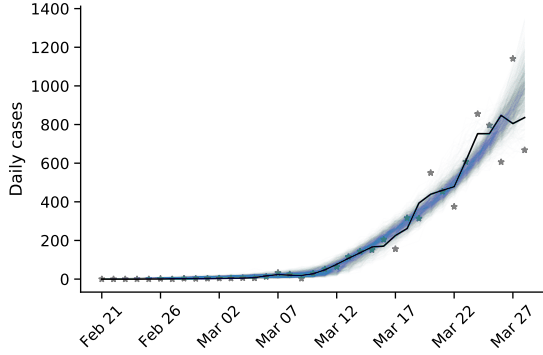
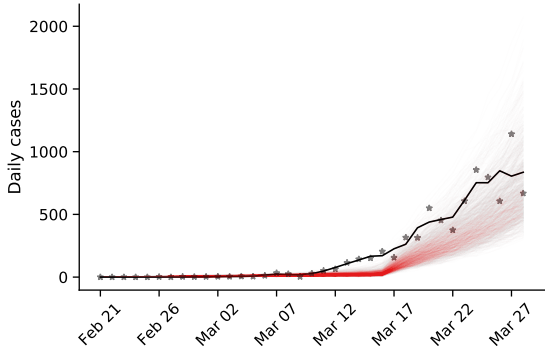
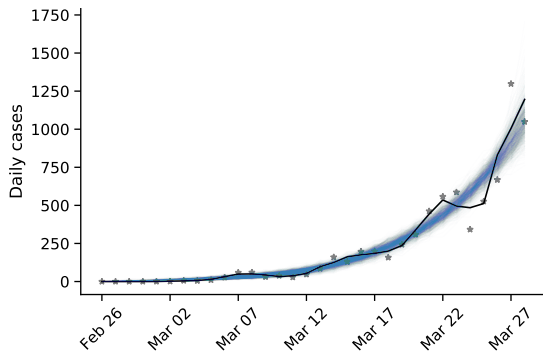
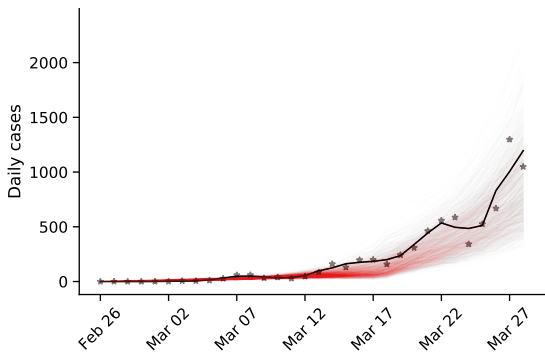


Figure S2: Effective date of non-pharmaceutical interventions in Switzerland matches the official date
 Posterior distribution of τ , the effective start date of NPI, is shown as a histogram of MCMC samples. Red line shows the official last NPI date τ^* . Black line shows the estimated $\hat{\tau}$. Shaded area shows a 95% credible interval (area in which $P(|\tau - \hat{\tau}| \mid \mathbf{X}) = 0.95$).

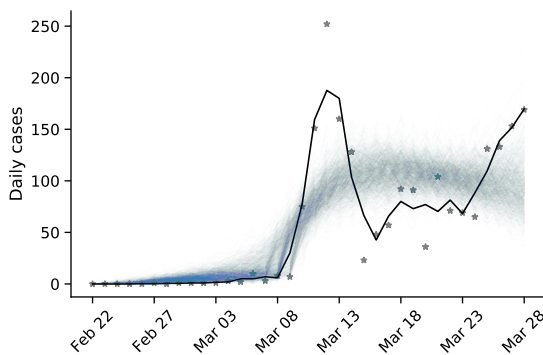
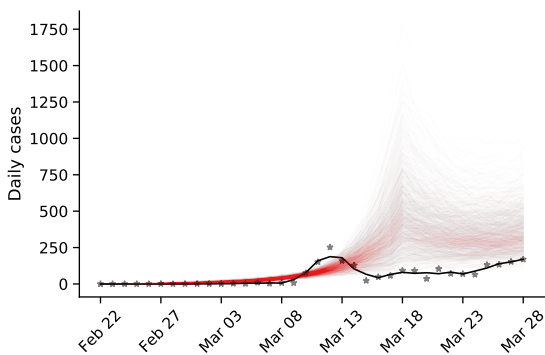
Austria



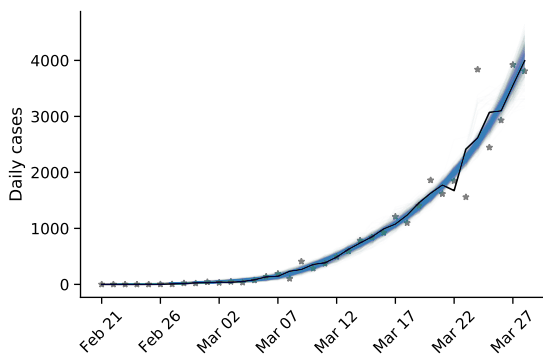
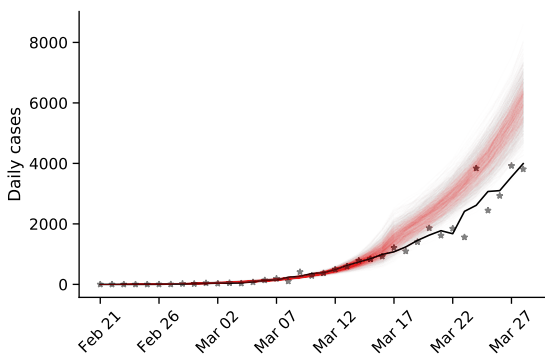
Belgium



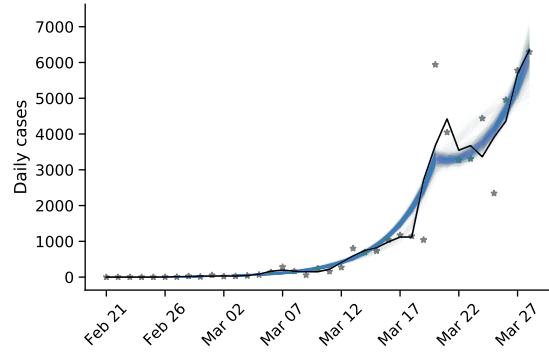
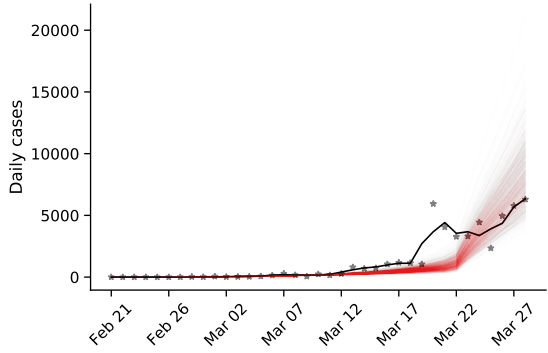
Denmark



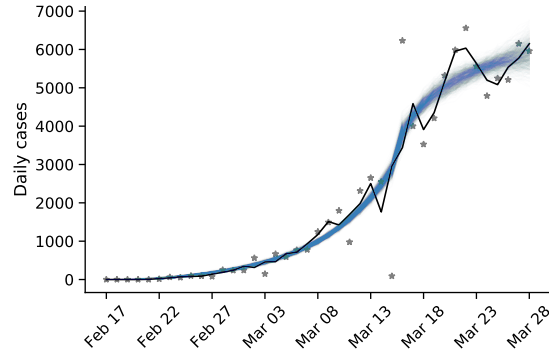
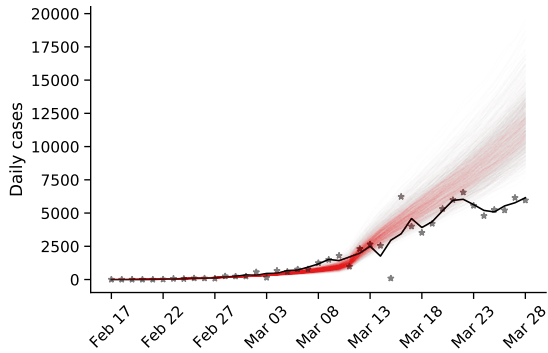
France



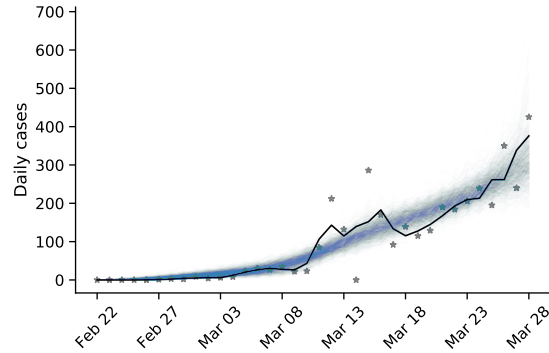
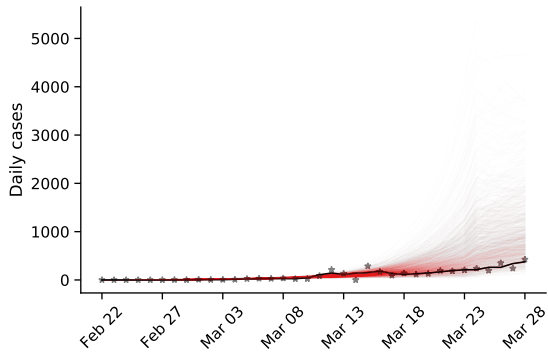
Germany



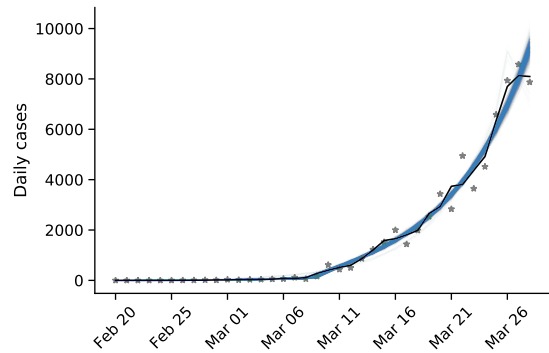
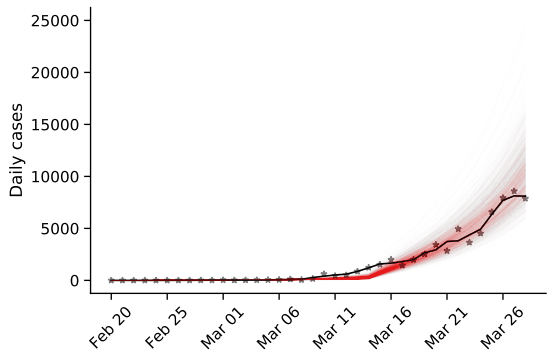
Italy



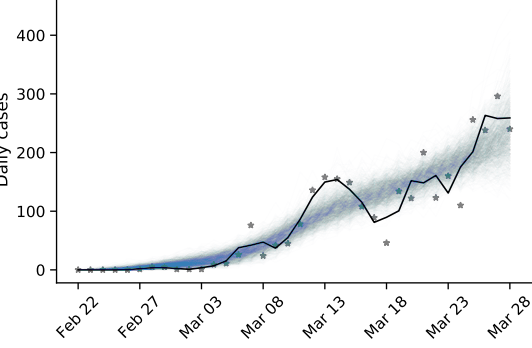
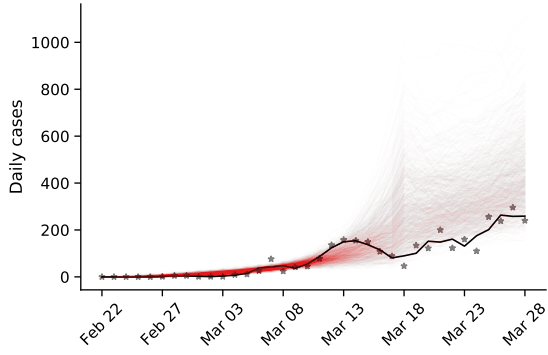
Norway



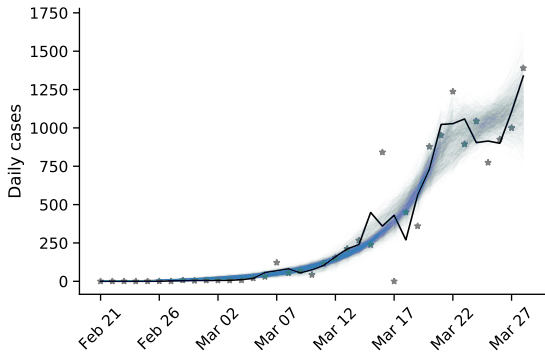
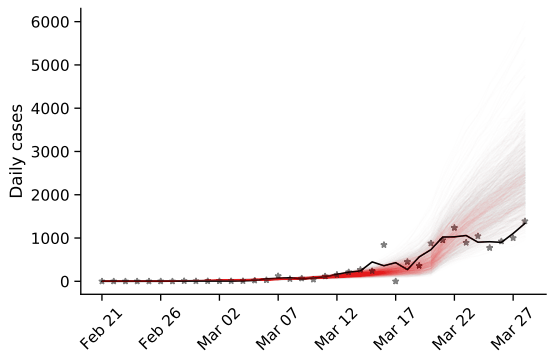
Spain



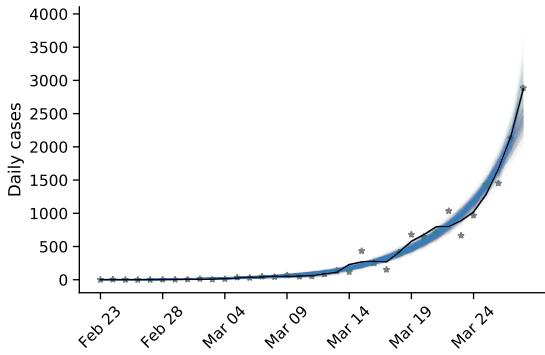
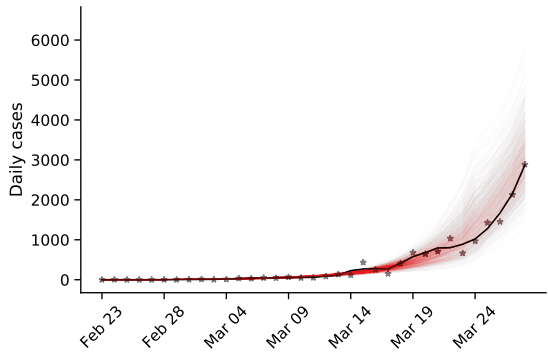
Sweden



Switzerland



United Kingdom



Wuhan, China

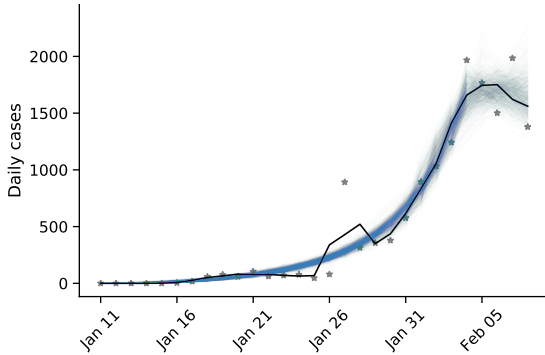
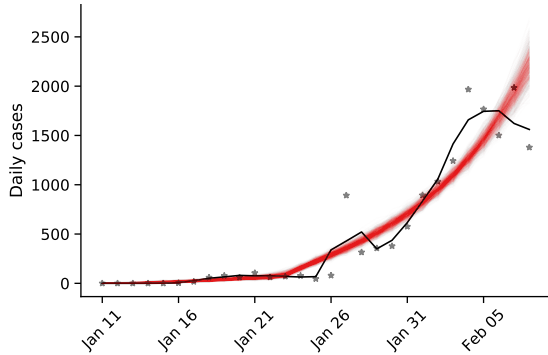


Figure S3. Posterior prediction check plots Markers represent data (\mathbf{X}). Black line represent a smoothing of the data points using a Savitzky-Golay filter. Color lines represent posterior predictions from a model with fixed τ , in red, and free τ , in blue. These predictions are made by drawing 1,000 samples from the parameter posterior distribution and then generating a daily case count using the SEIR model in Eq. (1). Note the differences in the y-axis scale.